Even-parity autoionizing states in the extreme-ultraviolet photoabsorption spectra of Mg, Al^+, and Si^{2+}

J. P. Mosnier, J. T. Costello, E. T. Kennedy, L. Kiernan, and M. H. Sayyad
School of Physical Sciences, Dublin City University, Glasnevin, Dublin 9, Ireland
(Received 12 July 1993)

The dual-laser-produced plasma (DLP) photoabsorption technique has been used to study $2p \rightarrow 3s$ excitations in the isoelectronic species Mg, Al^+, and Si^{2+} prepared in the excited configuration $2p^6 3s 3p$. The autoionizing upper states belong to the $2p^5 3s^2 3p$ even-parity configuration. The versatility of the technique is demonstrated through a careful combination of space- and time-resolved photoabsorption scans. Plasma conditions optimized for the observation of the inaccessible parity regime were successfully reproduced along the isoelectronic sequence of interest. All the observed transitions were interpreted with the help of multiconfigurational atomic structure calculations. In the case of magnesium, the photoabsorption data are compared with the ejected-electron spectra excited by low-energy electron impact of Pejcev *et al.* [J. Phys. B **10**, 2389 (1977)].

PACS number(s): 32.30.Jc, 32.70.−n

I. INTRODUCTION

Experimental data on inner-shell photoexcitation or photoionization in neutral, singly, or multiply ionized atoms are required for the understanding of many laboratory plasma and astrophysical phenomena. As atoms in a condensed-matter matrix often exist in ionic form, photoabsorption measurements on free ions can additionally prove very helpful in interpreting solid-state spectra. Systematic investigations along isoelectronic or isonuclear sequences are of particular value as they provide insight into fundamental aspects of the photoionization process such as relativistic effects, correlation effects, and orbital collapse, see, e.g., [1,2]. Due to their selective nature, photoion [3] and especially photoelectron experiments [4] carried out by crossing or merging ion beams with monochromatized synchrotron radiation constitute the most powerful tools for the probing of the photoionization process. Due mostly to the severe experimental difficulties inherent in the production of an ion beam of sufficiently high density, the number of cross-section measurements has remained low to date. The setting up of advanced ion sources at the site of third generation synchrotron light sources will eventually make it possible to carry out with singly or multiply charged ions photoionization experiments comparable to those currently carried out with neutral beams [5].

Laser-driven inner-shell photoabsorption experiments, namely, resonant laser-driven ionization [6] or dual-laser plasma (DLP) [7], provide total cross-section data usually on a relative rather than an absolute scale. In these laboratory-based experiments, the source of continuum background is the radiation emitted by a vacuum spark discharge or a laser-produced plasma and the absorbing medium is a plasma. The DLP technique has proven to be the most versatile for the study of a wide range of ions, see, e.g., [8,9] and neutral species, see, e.g., [10]. A complete account giving detailed descriptions of the various instrumental developments as well as the results obtained with this technique can be found in a recent review article by Costello *et al.* [11] and we refer the reader to this paper and all the references therein for more detailed information (see also Ref. [5]). One feature of the DLP technique is that it is possible to form an ionized plasma of any material element by focusing the output of a high power pulsed laser onto a target slab made of that element. The average ionization of the plasma will depend mostly on the incident laser power density. Also, the ionic densities obtained in laser-driven experiments are orders of magnitude larger than those achieved in the synchrotron ion beam experiments mentioned above. Laser-driven experiments can therefore provide essential atomic data for ions which will subsequently be used in detailed quantitative synchrotron-based experiments. The recently published study of the resonant photoionization of the $4s$ electron in Ca^+ [4] has clearly illustrated this heuristic property.

One particularly important aspect in the study of the many electron dynamics of core excited atoms is concerned with the study of species which have been prepared beforehand in a specific state resulting from the excitation of (usually) one outer-shell electron. Thus the autoionization of atomic states that do not connect to the ground state via the electric dipole operator can be investigated. Such experiments were carried out in the inner-shell regime first using photoabsorption spectroscopy [12,13] and then using photoelectron spectroscopy [14]. Also, the controllable excitation of a valence electron into higher states offers the unique opportunity to produce gradual modifications in the effective potential of an inner-shell electron [15,16]. The specific properties of high-intensity synchrotron light sources (wigglers, undulators) combined with highly selective excitation mechanisms and detection techniques have initiated measurements on excited atoms providing an ever more complete description of the photoionization process, e.g., resonant photoionization of excited aligned species [17], direct photoionization cross sections of excited atoms [18], and

angular dependence of ejected electrons in the photoionization of excited aligned atoms [19].

In all the experiments mentioned above, the excitation technique used is based on the pioneering works of Bradley [20,21] and of McIlrath and Carlsten [22,23]: a high power tunable dye laser selectively pumps a ground-state atomic vapor into an excited state. The population density of the excited state thus obtained is large enough so as to make a photoabsorption or a photoelectron spectrum originating from it readily observable. The applicability of the technique to a wide range of atomic species is only limited by the tuning range of the high power dye laser. As the spectral range covered by currently available high power dye lasers is limited to the visible region, excited-state studies have been restricted to only a few alkali and alkaline-earth elements to date.

In a hot and dense medium, such as a laser-produced plasma, the situation is somewhat different and may, at first sight, seem to be almost inextricable. In effect, a complex combination of various collisional and recombination processes results in a spatial and temporal distribution of ions among different ionization states and excitation states. Mappings of the ionic composition of expanding laser-produced plasmas have been reported by several authors [24,25] using emission spectroscopy techniques. It is this transient nature of a laser-produced plasma that is exploited in the DLP photoabsorption technique: by careful combination of time and space scans it is possible to isolate almost exclusively one particular ionization state (including the neutral species) in its ground electronic state, see, e.g., [26]. In the present paper we show that (i) the inner-shell photoabsorption spectrum of an ion in a particular excited optical level can also be obtained using the DLP technique. The experimental procedure consists in finding the spatial and temporal conditions in which the population density of that excited state is maximum, i.e., the corresponding photoabsorption signal is maximized. (ii) The use of a laser plasma as a source of ions allows a systematic investigation of such conditions along an isoelectronic sequence. Obviously, a sizable population of ions in a particular excited state can only exist if the plasma conditions (density, temperature) are compatible with the detailed atomic energy level structure of the ion in question.

II. EXPERIMENT

We purposely do not give in the present paper any detailed description of the experimental facility which is now fully operational in our laboratory at Dublin City University as this will be done in a forthcoming paper [27]. We shall restrict ourselves here to a brief outline of the essential features of the system. Three synchronized high power lasers are available: a 1.5-J, 30-ns, Q-switched ruby laser, a 1-J, 15-ns, Q-switched Nd-YAG laser (where YAG denotes yttrium aluminum garnet), and a 2-J, 0.8-μs flashlamp pumped dye laser. The laser pulse delivered by the Nd-YAG laser is focused onto a tungsten rod in a vacuum chamber and the broadband extreme ultraviolet (XUV) radiation emitted by the plasma created at the focus is used to backlight a second plasma created by either the ruby or the dye laser. The second (fore) plasma constitutes the absorbing medium. Only the ruby laser was used in the present experiments and focusing was via a cylindrical lens (line plasma) in the case of magnesium and singly ionized aluminum and a spherical lens (point plasma) in the case of doubly ionized silicon. The Nd-YAG and the ruby lasers were synchronized with a multichannel digital delay system providing delays in the range 0–999.99 μs. The jitter between the two pulses is intrinsically limited by the firing electronics of the ruby laser and is better than ± 30 ns. A specially designed grazing incidence gold-coated toroidal mirror gathers the radiation transmitted by the absorbing plasma and focuses it onto the entrance slit of a 2.2-m grazing incidence UHV monochromator. The entrance slit width was kept at 10 μm in the present experiments. Detection of the dispersed radiation is by means of an XUV sensitive linear array detector. Data were acquired in the following manner. By firing the Nd-YAG laser only, the background continuum spectrum (I_0) is obtained. With both lasers firing the transmitted intensity (I) is recorded. Typically 20 such single shot spectra were acquired and numerically averaged to improve the signal-to-noise ratio of both I and I_0. The quantity $-\ln(I/I_0)$ was subsequently computed. A check for emission from the front plasma in the spectral range of interest was carried out by solely firing the ruby laser. Such XUV emission was found to be negligible here. For each setting of the array detector, a wavelength reference spectrum was also taken. Tabulated emission lines belonging to the Al V, Al VI, Al VII, O IV, O V, and O VI spectra were used for calibration purposes [28]. A standard third-order polynomial fitting procedure was applied to the reference spectrum in order to provide calibrated energy scales for the photoabsorption data. The energy uncertainty on a sharp photoabsorption line is thus equal to ± 0.01 eV in the case of Mg, ± 0.03 eV in the case of Al^+, and ± 0.05 eV in the case of Si^{2+}.

III. RESULTS AND DISCUSSION

Photoionization of the $3s$ and $2p$ subshells of atomic magnesium in its ground state has been the subject of a number of thorough experimental and theoretical studies, see [29] and all the references cited in these papers for prior literature. All these studies emphasize the importance of electron correlations, e.g., role of double-electron excitations, strength of satellite photoemission lines, etc.

In the present work, we have investigated the optimum experimental conditions, i.e., position (x) of the absorbing target and time delay (t) between the two laser pulses, for the observation of the $2p \rightarrow 3s$ photoabsorption spectrum of the isoelectronic species Mg, Al^+, and Si^{2+} in the excited states $2p^6 3s 3p\ ^1P$ and ^3P. The $3s3p\ ^1P$ (^3P) levels (neglecting fine structure) are located approximately 4.3 (2.7), 7.4 (4.6), and 10.3 eV (6.5 eV) above the ^1S ground state [30]. The electron configuration of the core excited states of the neutral is $2p^5 3^2 3p$. The corresponding even-parity states can autoionize via direct electrostatic interaction into either the $2p^6 3p\epsilon l$ or the $2p^6 3s\epsilon' l''$ continua. In the first type of decay if $\epsilon l = \epsilon p$, the $3p$ elec-

tron remains a spectator during the decay of the core excited states. In the second type of decay $\epsilon' l'' = \epsilon' s$ or $\epsilon' d$, the $^{3,1}P$ upper states can decay only radiatively in a pure LS coupling picture and the $3p$ electron participates in the decay of the inner hole.

The observed spectra are presented in Figs. 1(a)–1(c) (Mg, Al^+, and Si^{2+}, respectively, from top to bottom). The optimum values for the position (x) of the absorbing target surface with respect to the optic axis of the system and for the time delay (t) between the two laser pulses are indicated on each spectrum.

First, we note that a strong pair of resonances is present on the high-energy side of each spectrum. These lines are easily recognized as the $2p^6 3s\ ^2S_{1/2} \rightarrow 2p^5 3s^2\ ^2P_{1/2,3/2}$ transitions in the sodiumlike structure [31,32] and indicate that in the conditions of Fig. 1 a large fraction of ions exist in the ground state of the Na-like species. The remainder of the absorption lines in the spectra correspond to $2p^6 3s 3p \rightarrow 2p^5 3s^2 3p$ excitations and clearly break into two distinct groups which reflect the large exchange separation of $2p^6 3s 3p\ ^3P$ from $2p^6 3s 3p\ ^1P$. Note the longer value of time delay which had to be used in the case of the Mg spectrum, necessary in order to obtain an observable fraction of neutrals.

We note that the higher-energy lines associated with the ^3P initial state are in each case more intense than the lower-energy lines associated with the ^1P initial state (see Fig. 1). In view of the dynamical nature of the absorbing medium used and the time-resolved nature of our spectra, an interpretation of the observed relative intensity pattern would only be obtained with the help of an extensive model that would include the absorption strengths of the transitions involved together with a knowledge of the temporal and spatial development of the absorbing plasma plume, e.g., population and depopulation mechanisms of the ^3P and ^1P lower states. As such modeling entails developments outside the scope of the present paper, we shall not dwell on the interpretation of the relative intensities observed in Fig. 1. We note, however, that in the experimental conditions of Fig. 1 the gross features of the three spectra are similar, thereby indicating similar plasma dynamics and atomic physics for all three species. We shall expand on the latter point in the final sections of the paper.

Line measurements together with term assignments are listed in Table I. The computed transition energies and corresponding gf (weighted oscillator strength) values were obtained with the help of multiconfigurational atomic structure calculations [33]. The $2p^6 3s 3p$, $2p^6 3p 3d$, $2p^5 3s^2 3p$, $2p^5 3s 3p 3d$, and $2p^5 3p 3d^2$ electron configurations were included. No scaling of the various F, G, and R integrals and spin-orbit parameters was used.

We first consider the transitions having ^3P as initial state. The theoretical values listed in Table I are the *ab initio* computed values. Line assignments are straightforward in this case as the computed values are in very good agreement with the measured values. In the case of transitions having ^1P initial state, it was found that the *ab initio* computed transition energies differed from the measured values by a constant amount roughly equal to 0.5 eV in all three spectra. This is due to an overestimation of the $G^1(3s,3p)$ exchange integral. Although an abundant literature is available on the subject of the precise calculation of the optical levels in the magnesium series (see, e.g., [34]), it was found sufficient of the purpose of assigning inner-shell transitions to apply a constant correction factor to the relevant transition energies. The value of the correction is equal to the amount that must be added

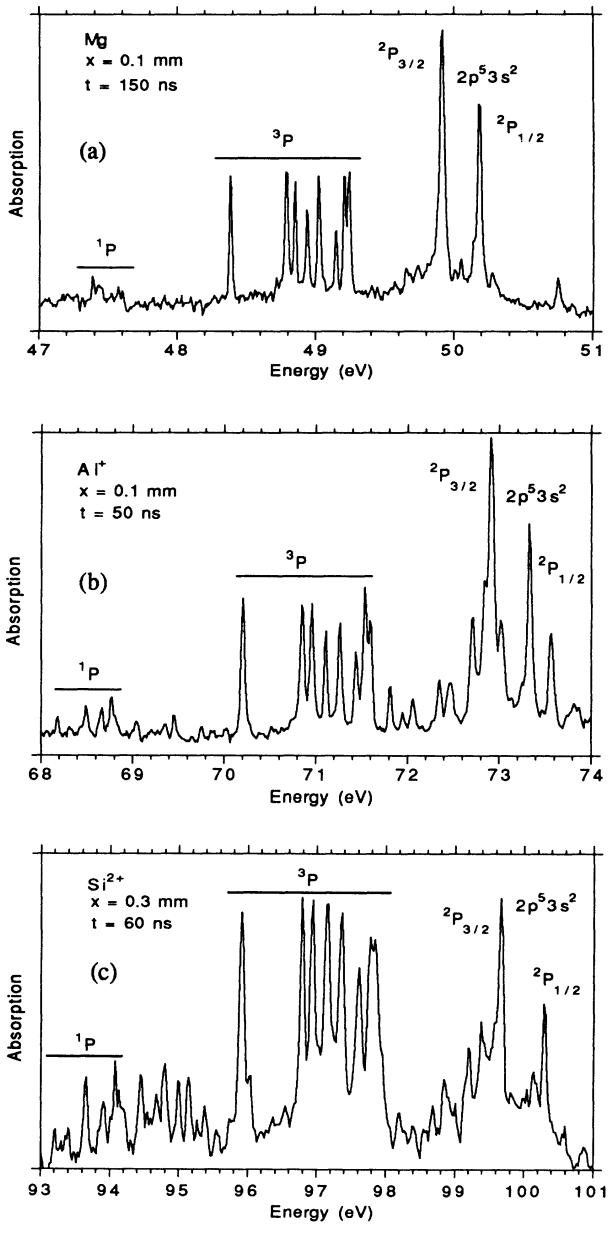

FIG. 1. The relative photoabsorption spectra of Mg (a), Al^+ (b), and Si^{2+} (c) in the region of the $2p^6 3s 3p\ ^{3,1}P \rightarrow 2p^5 3s^2 3p\ ^{3,1}L$ transition array as obtained with DLP photoabsorption technique. The optimum values for the position of the absorbing target (x) and time delay (t) between the two laser pulses are indicated on each spectrum. The spectral intervals for the transitions having $2p^6 3s 3p\ ^3P$ or ^1P as initial state are delineated in each spectrum. Also marked in each spectrum are the $2p^5 3s^2\ ^2P_{1/2,3/2}$ resonances in the sodiumlike ion.

to the *ab initio* energy value of $2p^6 3s 3p\ ^1P$ in order to make the ^3P-^1P energy interval exactly equal to its tabulated value [30]. This factor is equal to 5796 cm^{-1} (Mg), 4845 cm^{-1} (Al^+), and 4462 cm^{-1} (Si^{2}). This simple constant shifting procedure brings the calculated values in good agreement with the measured ones; the only exception being the $^1P_1$-$^1S_0$ transitions which are not present in our spectra. In view of the general good agreement previously observed for all levels except $2p^5 3s^2 3p\ ^1S_0$, we surmise that our *ab initio* unscaled calculations provide only a mediocre description of the wave function of the latter. Thus the corresponding transition energies and strengths quoted in Table I are only indicative. This view is supported by the interpretation of the photoinduced $2p$ Auger spectrum of atomic aluminum by Malutzki *et al.* [35] in which similar difficulties are reported and discussed in the case of the calculation of the Auger decay rate of $2p^5 3s^2 3p\ ^1S_0$.

In a pure *LS* coupling picture, the $2p^6 3s 3p \rightarrow 2p^5 3s^2 3p$ spectrum exhibits the characteristic $^{3,1}P \rightarrow {}^{3,1}S, {}^{3,1}P, {}^{3,1}D$ structure with cross-system transitions being forbidden. However, the observed spectra are more complex than suggested by this picture as a number of strong lines must be assigned to *LS* forbidden transitions (see Table I). Comparison with the $2p$ valence excited photoabsorption spectra in the sodium sequence provides a straightforward explanation for this observation. In effect, it has been reported by several authors [36,37] that the structure of the $2p^6 3p \rightarrow 2p^5 3s 3p$ spectrum is due mostly to large spin-orbit mixing of different terms of the upper configuration produced by the $2p^5$ open core. It is plain that the addition of an extra electron in the $3s$ subshell should only be marginal in this respect and we therefore expect strong departure from *LS* coupling for some of the terms of the $2p^5 3s^2 3p$ configuration. Wave-function compositions of the $2p^5 3s^2 3p$ triplet and singlet states in Mg, Al^+, and Si^{2+} are given in Table II in increasing order of energy. Complete breakdown of *LS* coupling is exemplified by the almost complete mixing between $^3P_2$ and $^1D_2$. Indeed, for the three species considered, the levels labeled $^1D_2$ have a $^3P_2$ component of the order of 0.5 and the levels labeled $^3P_2$ have a $^1D_2$ component of the order of 0.4. Also, the $^1P_1$ levels are placed below the $^3P_1$ levels as a result of strong mixing between them. On the contrary, we note that the $^3S_1$, $^3D_3$, $^3P_0$, and $^1S_0$ are all 95% or more *LS* pure. Correlation mixing with

TABLE I. Measured energies, calculated energies, and gf values for the $2p^6 3s 3p\ ^{3,1}P - 2p^5 3s^2 3p\ ^{3,1}L$ transitions in Mg, Al^+, and Si^{2+}.

	Mg			Al^+			Si^{2+}		
Transition	Measured (eV)	Calculated (eV)	gf[a]	Measured (eV)	Calculated (eV)	gf[a]	Measured (eV)	Calculated (eV)	gf[a]
$^3P_2$-$^3S_1$		48.202	0.0324		70.211	0.0315		95.964	0.0298
$^3P_1$-$^3S_1$	48.38	48.406	0.0317	70.21	70.223	0.0314	95.99	95.993	0.0316
$^3P_0$-$^3S_1$		48.407	0.0132		70.231	0.0133		96.008	0.0138
$^3P_2$-$^3D_3$	48.79	48.752	0.191	70.86	70.812	0.206	96.80	96.803	0.2157
$^3P_2$-$^3D_2$		48.812	0.0110		70.905	0.0115		96.924	0.0105
$^3P_1$-$^3D_2$	48.85	48.816	0.102	70.97	70.917	0.1155	96.95	96.954	0.1226
$^3P_2$-$^3D_1$		48.907	0.0004		71.052	0.0004		97.144	0.0007
$^3P_1$-$^3D_1$		48.911	0.0125		71.064	0.0152		97.175	0.0147
$^3P_0$-$^3D_1$	48.94	48.912	0.0547	71.12	71.072	0.0613	97.16	97.182	0.0651
$^3P_2$-$^3P_2$	49.02	48.993	0.0429	71.27	71.223	0.0542	97.36	97.388	0.0653
$^3P_1$-$^3P_2$		48.996	0.0358		71.235	0.0370		97.419	0.0391
$^3P_2$-$^1P_1$		49.129	0.0147		71.416	0.0182		97.664	0.0205
$^3P_1$-$^1P_1$	49.14	49.133	0.0290	71.44	71.428	0.0307	97.62	97.688	0.0340
$^3P_0$-$^1P_1$		49.135	0.0009		71.432	0.0001		97.703	0.0002
$^3P_2$-$^3P_2$	49.20	49.177	0.0879	71.54	71.498	0.0975	97.77	97.803	0.1016
$^3P_1$-$^3P_2$		49.180	0.0001		71.511	0.0000		97.826	0.0000
$^3P_1$-$^3P_0$		49.193	0.0286		71.527	0.0336		97.826	0.0369
$^3P_2$-$^3P_1$	43.24	49.226	0.0340	71.60	71.577	0.0371	97.84	97.904	0.0400
$^3P_1$-$^3P_1$		49.229	0.0085		71.589	0.0104		97.927	0.0112
$^3P_0$-$^3P_1$		49.231	0.0141		71.593	0.0166		97.934	0.0176
$^3P_1$-$^1S_0$		50.973	0.0001		75.097	0.0001		102.349	0.0002
$^1P_1$-$^3S_1$		46.766	0.0005		67.415	0.0004		92.271	0.0004
$^1P_1$-$^3D_2$	47.20	47.175	0.0236	68.19	68.139	0.0229	93.20	93.229	0.0252
$^1P_1$-$^3D_1$	47.31	47.270	0.0133	68.44	68.440	0.0098	93.40	93.447	0.0095
$^1P_1$-$^3P_2$	47.39	47.355	0.0618	68.49	68.458	0.0726	93.65	93.694	0.0749
$^1P_1$-$^1P_1$	47.52	47.493	0.0348	68.67	68.648	0.0330	93.92	93.971	0.0294
$^1P_1$-$^3P_2$	47.57	47.540	0.0525	68.77	68.732	0.0647	94.08	94.106	0.0741
$^1P_1$-$^3P_0$		47.553	0.0002		68.751	0.0002		94.106	0.0003
$^1P_1$-$^3P_1$	47.60	47.588	0.0254	68.81	68.812	0.0246	94.14	94.206	0.0237
$^1P_1$-$^1S_0$		49.333	0.0345		71.913	0.0554		98.628	0.0714

[a]Weighted oscillator strength.

TABLE II. Calculated purity of the levels (in increasing order of energy) of the $2p^5 3s^2 3p$ configuration in Mg, Al^+, and Si^{2+}.

	$^3D_3$			$^3D_2$			$^3D_1$			$^3P_2$			$^3P_1$			$^3P_0$			$^1D_2$			$^1P_1$			$^3S_1$			$^1S_0$		
Level	Mg	Al^+	Si^{2+}	Mg	Al^+	Si^{2+}	Mg	Al^+	Si^{2+}	Mg	Al^+	Si^{2+}	Mg	Al^+	Si^{2+}	Mg	Al^+	Si^{2+}	Mg	Al^+	Si^{2+}	Mg	Al^+	Si^{2+}	Mg	Al^+	Si^{2+}	Mg	Al^+	Si^{2+}
$^3S_1$																									95	95	95			
$^3D_3$	98	97	97																											
$^3D_2$				78	79	78													17	14	14									
$^3D_1$							70	74	73				10	8	10				44	44	41	18	14	15						
$^1D_2$							27	22	24	51	51	54	25	27	27							46	47	46						
$^1P_1$				17	16	17				43	42	39				97	96	96	37	39	41									
$^3P_2$													62	59	59							33	35	36						
$^3P_0$																												97	95	95
$^3P_1$																														
$^1S_0$																														

$2p^5 3s 3p 3d$ amounts to 1.5% at most and therefore has a minor influence over the energy level structure of the $2p^5 3s^2 3p$ configuration. On the other hand, when one considers autoionization or Auger decay, it is well known that such configuration effects play an essential role in the understanding of the origin of satellite features attributed to electron correlations (see below for further discussion).

Following our previous conclusions regarding the relative intensity patterns in Fig. 1 (see above), we infer from Fig. 1 and Table II that on going from Mg to Si^{2+}, the dominant effect remains spin-orbit mixing due to the open core since the increase in nuclear charge has little influence on the restructuring of the energy level system of the $2p^5 3s^2 3p$ configuration. This is in sharp contrast with the behavior of the $2p^5 3s^2 3d$ configuration observed in photoabsorption along the same isoelectronic sequence [38].

Further insight into the dynamics of autoionizating states can be obtained from the study of the decay processes of such states. A resonant photoemission study of laser-excited magnesium atoms and magnesiumlike ions, for instance, would provide valuable information to complement the present photoabsorption data, however, to the best of our knowledge no such data exist in the literature.

An extensive study of the ejected-electron spectrum of magnesium autoionizing levels excited by low-energy electron impact was published some years ago by Pejcev *et al.* [39]. At the low incident electron energies (62, 100, and 400 eV) used by these authors, the $2p^5 3s^2 3p$ autoionizing levels get populated via quadrupole excitation of a $2p$ ground-state electron. Although the presence of these levels was mentioned no assignments were given. We use our photoabsorption data, together with the values of the known optical energy levels of Mg and Mg^+ (Martin and Zalubas) [30] in order to predict the kinetic energies of the electron ejected upon autoionization and compare the values thus obtained with those measured by Pejecev *et al.* with a quoted energy resolution of 0.035 eV and an energy uncertainty of 0.015 eV [39]. We perform these calculations for both the $2p^6 3p$ (12.072 eV) and the $2p^6 3s$ (7.646 eV) final states of the decay in Mg^+. The results are summarized in Table III. We observe that there is excellent agreement (within 0.02 eV) between our predicted data and the ejected electron lines numbered 26, 27, 29, 30, 31, and 32 in [39]. Also we note that the intensity of this group of lines is stronger at lower incident electron energy. We therefore conclude that this group of lines is due to the autoionizating decay of the $2p^5 3s^2 3p\,^{3,1}P, ^{3,1}D$ states into the corresponding $2p^6 3p\epsilon l$ continua. In the case of the decay $2p^5 3s^2 3p\ ^3S_1 \rightarrow 2p^6 3p$, we predict an energy of 39.02 eV for the ejected electron. No such line is present in Ref. [39]. Therefore, assuming statistical population of the initial states by electron impact, the autoionization transition probability of the $2p^5 3s^2 3p\ ^3S_1$ state into the $2p^6 3p\epsilon l$ continuum appears to be substantially smaller than that of the $2p^5 3s^2 3p\ ^{3,1}P, ^{3,1}D$ states into the corresponding $2p^6 3p\epsilon l$ continua and the ejected-electron line is therefore too weak to be observed in the experimental conditions of Ref. [39]. We note that the

same situation is also encountered in the photoinduced $2p$ Auger spectrum of atomic aluminum [35]. It was suggested in Ref. [39] that the lines numbered 43, 44, and 45 (the intensities of which exhibit the same pattern of behavior as lines 26, 27, 29, 30, 31, and 32 when the energy of the incident electron beam is varied) appear to be due to the excitation of nonoptical Mg I states which subsequently decay to $2p^6 3s$. This is confirmed by our photoabsorption measurements, the agreement in energy being within 0.02 eV for the three lines. The corresponding decays are $2p^5 3s^2 3p\ ^3D_{1,2,3} \rightarrow 2p^6 3s$.

The dependence of the intensity of the ejected-electron line numbered 40 (43.41 eV) in Ref. [39] upon the energy of the low-energy incident electron beam suggests the assignment $2p^5 3s^2 3p\ ^3S_1 \rightarrow 2p^6 3s$ for the corresponding autoionizating decay (see Table III). The ejected-electron lines numbered 46 (44.17 eV), 47 (44.25 eV), and 48 (44.32 eV) are possible candidates for the decay of the $2p^5 3s^2 3p$ states having dominant ^3P or ^1P character (Table III). The assignments are considered less definite in these cases for the dependence on incident energy differs appreciably for the three lines as discussed in [39].

According to our data autoionization decays of $2p^5 3s^2 3p$ to $2p^6 3d$ (16.510 eV) and $2p^6 4p$ (17.643 eV)—entirely due to electron correlations—would give rise to ejected electrons with kinetic energies in the 34.585–35.44 and 33.452–34.311 eV ranges, respectively. In the first case the presence of the very intense $L_{2,3}M_1M_1$ Auger lines at 34.86 and 35.13 eV makes the identification of the corresponding ejected-electron lines impossible in the spectrum of Pejcev *et al.* [39]. A different experimental technique would be required in this case to clarify this important point, i.e., the strength of electron correlations which result in $2p^6 3d$ as the final state of the autoionizing decay of $2p^5 3s^2 3p$. There is no evidence in Ref. [39] for the presence of ejected electrons with kinetic energies corresponding to the second type of decay ($2p^6 4p$ final state) for which a possible class of correlation effects would be $3p \rightarrow 4p$ shakeup excitation. We note that in the case of the photoinduced $2p$ Auger spectrum of atomic aluminum [35], the $2p^6 3d$ exit channel contributes about 15% of the overall intensity whereas $2p^6 4p$ has a negligible contribution.

Finally, we point out that in the spectrum of Pejcev *et al.* [39] the group of lines we assigned to the $2p^5 3s^2 3p \rightarrow 2p^6 3p$ decay is stronger than the group of lines we assigned to the $2p^5 3s^2 3p \rightarrow 2p^6 3s$ decay, with, however, the notable exception of the lines corresponding to the decay of $2p^5 3s^2 3p\ ^3S_1$ in which case the opposite situation is observed. This seems to suggest that the $3p$ electron chiefly remains a spectator during the autoionizing decay of the $2p^5 3s^2 3p\ ^{3,1}P, ^{3,1}D$ states resulting in $2p^6 3p\epsilon l$ as a preferential decay channel.

IV. CONCLUSIONS

In conclusion, we have shown that the dual-laser plasma photoabsorption technique can be specifically applied to the study of the inner-shell excitation spectra of neutral, singly, and doubly ionized atomic species prepared in energy states corresponding to the excitation of one valence electron. This is presently the only experimental

TABLE III. Energies of the electrons ejected upon autoionization decay of $2p^5 3s^2 3p\ ^{3,1}L$ states in magnesium.

		Ejected-electron energy (eV)	
Excited-state energy[a] (eV)	Autoionization transition	Predicted[b]	Ref. [39][c]
51.09	$2p^5 3s^2 3p\ ^3S_1 - 2p^6 3p$	39.02	
	$-2p^6 3s$	43.45	43.41 (40)
51.50	$2p^5 3s^2 3p\ ^3D_3 - 2p^6 3p$	39.43	39.43 (26)
	$-2p^6 3s$	43.85	43.85 (43)
51.56	$2p^5 3s^2 3p\ ^3D_2 - 2p^6 3p$	39.49	39.50 (27)
	$-2p^6 3s$	43.92	43.90 (44)
51.65	$2p^5 3s^2 3p\ ^3D_1 - 2p^6 3p$	39.58	39.60 (29)
	$-2p^6 3s$	44.00	43.97 (45)
51.73	$2p^5 3s^2 3p\ ^3P_2 - 2p^6 3p$	39.66	39.67 (30)
	$-2p^6 3d$[d]	44.09	44.17 (46)
51.86	$2p^5 3s^2 3p\ ^1P_1 - 2p^6 3p$	39.79	39.80 (31)
	$-2p^6 3s$[d]	44.21	44.25 (47)
51.91	$2p^5 3s^2 3p\ ^3P_2 - 2p^6 3p$	39.84	39.86 (32)
	$-2p^6 3s$[d]	44.27	44.25 (47)
51.92	$2p^5 3s^2 3p\ ^3P_0 - 2p^6 3p$	39.85	39.86 (32)
	$-2p^6 3s$[d]	44.28	44.25 (47)
51.95	$2p^5 3s^2 3p\ ^3P_1 - 2p^6 3p$	39.88	39.86 (32)
	$-2p^6 3s$[d]	44.31	44.32 (48)

[a]Obtained from the measurement of $2p^6 3s 3p\ ^3P \rightarrow 2p^5 3s^2 3p\ ^{3,1}L$ transitions and the energy level given in Ref. [30] for $2p^6 3s 3p\ ^3P$.

[b]Obtained from the excited-state energy column and the optical energy levels of Mg^+ given in Ref. [30].

[c]The number in parentheses is the line number as labeled in Ref. [39].

[d]Tentative assignment.

technique which allows such measurements in singly and doubly charged positive ions. We have carried out such a study along the magnesium isoelectronic sequence by measuring the $2p \rightarrow 3s$ photoabsorption spectra of Mg, Al^+, and Si^{2+} in the excited states $2p^6 3s 3p\ ^{3,1}P$ which give access to core excited states belonging to the optically forbidden $2p^5 3s^2 3p$ configuration.

We have also used our photoabsorption data in the case of atomic magnesium to interpret its ejected-electron spectrum excited by low-energy electron impact corresponding to the autoionization decay of $2p^5 3s^2 3p$ states. In this specific case, the only identified exit channels were $2p^6 3p$ and $2p^6 3s$ with the former appearing as a preferential decay channel for $2p^5 3s^2 3p$ states having $L \neq 0$.

ACKNOWLEDGMENTS

This work was supported by EOLAS (Irish National Science and Technology Agency) under Grant No. SC/91/120, the EC Science Programme under Grant No. SCI-0364, and by the Rutherford Appleton Laboratory under Contract No. CRAY03.

[1] T. B. Lucatorto, T. J. McIlrath, J. Sugar, and S. M. Younger, Phys. Rev. Lett. **47**, 1124 (1981).
[2] Jahanti Lahiri and Steven T. Manson, Phys. Rev. A **37**, 1047 (1988).
[3] B. Peart and C. Lyon, J. Phys. B **20**, L673 (1987).
[4] J. M. Bizau, D. Cubaynes, M. Richter, F. J. Wuilleumier, J. Obert, C. Putaux, T. J. Morgan, E. Kallne, S. Sorensen, and A. Damany, Phys. Rev. Lett. **67**, 576 (1991).
[5] F. J. Wuilleumier, in *Correlations and Polarization in Electronic and Atomic Collisions and (e,2e) Reactions,* edited by P. J. O. Teubner and E. Weigold, IOP Conf. Proc. No. 122 (Institute of Physics and Physical Society, Bristol, 1992), p. 203.
[6] T. B. Lucatorto and T. J. McIlrath, Phys. Rev. Lett. **37**, 428 (1976).
[7] A. Carillon, P. Jaegle, and P. Dhez, Phys. Rev. Lett. **25**, 140 (1970); P. K. Carroll and E. T. Kennedy, *ibid.* **38**, 1068 (1977).
[8] J. E. Hansen, J. Brilly, E. T. Kennedy, and G. O'Sullivan, Phys. Rev. Lett. **63**, 1934 (1989).
[9] P. Nicolosi, E. Jannitti, and G. Tondello, J. Phys. (Paris) Colloq. IV **1**, C1-89 (1990).
[10] J. T. Costello, E. T. Kennedy, B. F. Sonntag, and C. L. Cromer, J. Phys. B **24**, 5063 (1991).
[11] J. T. Costello, J-P. Mosnier, E. T. Kennedy, P. K. Carroll, and G. O'Sullivan, Phys. Scr. **34**, 77 (1991).
[12] T. B. Lucatorto and T. J. McIlrath, Phys. Rev. Lett. **38**, 1390 (1977).
[13] J. Sugar, T. B. Lucatorto, T. J. McIlrath, and A. W. Weiss, Opt. Lett. **4**, 109 (1979).
[14] J. M. Bizau, F. Wuillemier, D. L. Ederer, J. C. Keller, J. L. LeGouet, J.-L. Picque, B. Carre, and P. M. Koch, Phys. Rev. Lett. **55**, 1281 (1985).
[15] B. F. Sonntag, C. L. Cromer, J. M. Bridges, T. J. McIlrath, and T. B. Lucatorto, in *Short Wavelength Coherent Radiation: Generation and Applications* (Monterey, California, March 24–26, 1986), edited by D. T. Attwood and J. Bokor, AIP Conf. Proc. No. 147 (AIP, New York, 1986), p. 412.
[16] M. Ferray, F. Gounand, P. D'Oliveira, P. R. Fournier, D. Cubaynes, J. M. Bizau, T. J. Morgan, and F. J. Wuilleumier, Phys. Rev. Lett. **59**, 2040 (1987).
[17] M. Meyer, B. Muller, A. Nunnemann, Th. Prescher, E. v. Raven, M. Richter, M. Schmidt, B. Sonntag, and P. Zimmermann, Phys. Rev. Lett. **59**, 2963 (1987).
[18] D. Cubaynes, J. M. Bizau, F. J. Wuilleumier, B. Carre, and F. Gounand, Phys. Rev. Lett. **63**, 2460 (1989).
[19] M. Pahler, C. Lorenz, E. von Raven, J. Ruder, B. Sonntag, S. Baier, B. R. Muller, M. Schulze, H. Staiger, P. Zimmermann, and N. M. Kabachnik, Phys. Rev. Lett. **68**, 2285 (1992).
[20] D. J. Bradley, Appl. Opt. **8**, 1957 (1969).
[21] D. J. Bradley, P. Ewart, J. V. Nicholas, J. R. D. Shaw, and D. G. Thompson, Phys. Rev. Lett. **31**, 263 (1973).
[22] T. J. McIlrath, Appl. Phys. Lett. **15**, 41 (1969).
[23] T. J. McIlrath and J. L. Carlsten, J. Phys. B **6**, 697 (1973).
[24] F. E. Irons, R. W. P. McWhirter, and N. J. Peacock, J. Phys. B. **5**, 1975 (1972).
[25] F. Irrera, G. Tondello, and P. Nicolosi, Nuovo Cimento **7**, 626 (1986).
[26] J. T. Costello, D. Evans, R. B. Hopkins, E. T. Kennedy, L. Kiernan, M. W. D. Mansfield, J.-P. Mosnier, M. H. Sayyad, and B. F. Sonntag, J. Phys. B **25**, 5055 (1992).
[27] E. T. Kennedy *et al.* (unpublished).
[28] R. P. Kelly, J. Phys. Chem. Ref. Data **16**, Suppl. 1, 228 (1987).
[29] Pranawa C. Deshmukh and Steven T. Manson, Phys. Rev. A **28**, 209 (1983); A. Hausmann, B. Kammerling, H. Kossmann, and V. Schmidt, Phys. Rev. Lett. **61**, 2669 (1988); Zikri Altun, Phys. Rev. A **40**, 4968 (1989); S. B. Whitfield, C. D. Caldwell, and M. O. Krause, *ibid.* **43**, 2338 (1991); S. B. Whitfield, J. Tulkki, and T. Aberg, *ibid.* **43**, 6983 (1991); B. Kammerling, A. Hausmann, J. Lauger, and V. Schmidt, J. Phys. B **25**, 4773 (1992).
[30] W. C. Martin and R. Zalubas, J. Phys. Chem. Ref. Data **8**, 817 (1979); **9**, 1 (1980); **12**, 323 (1983).
[31] J. M. Esteva and G. Mehlman, Astrophys. J. **193**, 747 (1974).
[32] J.-P. Mosnier, J. Brilly, and E. T. Kennedy, J. Phys. (Paris) Colloq. **48**, C9-219 (1987).
[33] R.D. Cowan, *The Theory of Atomic Structure and Spectra* (University of California Press, Berkeley, 1981).
[34] A. Hibbert and F. P. Keenan, J. Phys. B **20**, 4693 (1987).
[35] R. Malutzki, A. Wachter, V. Schmidt, and J. E. Hansen, J. Phys. B **20**, 5411 (1987).
[36] C. Froese-Fisher, Phys. Rev. A **34**, 1667 (1986).
[37] J. Brilly, E. T. Kennedy, and J. P. Mosnier, Phys. Scr. **41**, 30 (1990).
[38] M. H. Sayyad, J. T. Costello, E. T. Kennedy, L. Kiernan, and J. P. Mosnier (unpublished).
[39] V. Pejcev, T. W. Ottley, D. Rassi, and K. J. Ross, J. Phys. B **10**, 2389 (1977).